

# Extracting a function encoded in amplitudes of a quantum state by tensor network and orthogonal function expansion

Koichi Miyamoto<sup>1,\*</sup> and Hiroshi Ueda<sup>1,2,3,†</sup>

<sup>1</sup>Center for Quantum Information and Quantum Biology, Osaka University, Toyonaka, Osaka 560-0043, Japan

<sup>2</sup>JST, PRESTO, Kawaguchi, Saitama 332-0012, Japan

<sup>3</sup>Computational Materials Science Research Team, RIKEN Center for Computational Science (R-CCS), Kobe 650-0047, Japan

(Dated: September 1, 2022)

There are some quantum algorithms on problems to find the functions satisfying the given conditions, such as solving partial differential equations, and they claim the exponential quantum speedup compared to the classical methods. However, they in general output the quantum state in which the solution function is encoded in the amplitudes, and reading out the function values as classical data from such a state can be so time-consuming that the quantum speedup is ruined. In this paper, we propose a general method to such a function readout task. We approximate the function by orthogonal function expansion. Besides, in order to avoid the exponential increase of the parameter number for the high-dimensional function, we use the tensor network that approximately reproduces the expansion coefficients as a high-order tensor. We present the quantum circuit that encodes such a tensor network-based function approximation and the procedure to optimize the circuit and obtain the approximating function. We also conduct the numerical experiment to approximate some finance-motivated function and observe that our method works.

## I. INTRODUCTION

Quantum computing is an emerging technology that is expected to provide the speedup for various classically time-consuming problems. Following its recent great advance, people are now investigating its practical applications. Some fundamental quantum algorithms have evolved to the solvers for more concrete numerical problems. For example, the Harrow-Hassidim-Lloyd (HHL) algorithm [1] to solve linear equation systems and its extensions [2–10] lead to the quantum solvers for ordinary differential equations (ODEs) [11–14] and partial differential equations (PDEs) [3, 15–19], including even nonlinear systems [20–25]. Then, the practical usage of these algorithms have been proposed in the various fields such as epidemiology [20, 26], fluid dynamics [20], and financial derivative pricing [27]. Compared with classical methods, these quantum algorithms achieve the exponential speedup with respect to the size of the problem, which means, in the ODE case, the number of equations in the system, and, in the PDE case, the dimension  $d$  of the domain of the solution function  $f$ , that is, the number of the variables of  $f$ . Thus, they are considered as the promising candidates for the killer applications of quantum computing. Also note that, in addition to the above algorithms that run on the fault-tolerant quantum computer (FTQC), there are also some algorithms on the noisy intermediate-scale quantum (NISQ) devices for solving ODEs and PDEs [28–42].

However, when we consider some quantum solvers including the above ones and the speedup they provide, we should pay attention to the meaning of the words “solve” and “speedup”. That is, we have to resolve the issue of *how to extract the function values from the quantum state*, which might ruin the quantum speedup.

The detail is as follows. As pointed out in [43], we should note that many quantum algorithms output not the solution as a figure, which we eventually want, but the quantum state in which the solution is encoded as the amplitudes. For example, the quantum algorithms for PDE solving output the quantum state in the form of  $|f\rangle := \frac{1}{C} \sum_{i=0}^{N_{\text{gr}}-1} f(\vec{x}_i) |i\rangle$ , where  $f$  is the solution function,  $\vec{x}_0, \vec{x}_1, \dots, \vec{x}_{N_{\text{gr}}-1}$  are the  $N_{\text{gr}}$  grid points in the domain of  $f$ ,  $|0\rangle, |1\rangle, \dots, |N_{\text{gr}}-1\rangle$  are the computational basis states, and  $C$  is the normalization factor. Then, the trouble is that reading out the values of the function as classical data from such a quantum state can be often the bottleneck. In the above example on PDE solving, the grid point number  $N_{\text{gr}}$  is exponentially large with respect to the dimension  $d$ : naively, taking  $n_{\text{gr}}$  grid points in each dimension leads to  $N_{\text{gr}} = n_{\text{gr}}^d$  points in total. This makes the amplitude  $\frac{1}{C} f(\vec{x}_i)$  of each basis state in  $|f\rangle$  exponentially small when the amplitude is not localized on certain grids. This means that, when we try to retrieve the amplitude and then the function value  $f(\vec{x}_i)$  at the point  $x_i$  by some method such as quantum amplitude estimation [44, 45], the exponentially large time overhead is added. Therefore, even if there is a quantum algorithm that generates the state  $|f\rangle$  exponentially faster than the classical algorithm outputs the value of  $f(\vec{x}_i)$ , obtaining  $f(\vec{x}_i)$  through the quantum algorithm might not be faster than the classical one.

If we want the function values at many points to, for example, know the functional form by plotting the values as a graph, the situation becomes worse. That is, naively, to obtain the function values at  $M$  points, we need to repeat the quantum algorithm  $M$  times.

Motivated by the above background, this paper focuses on how we can efficiently extract the function encoded as the amplitudes in the quantum state  $|f\rangle$ , given the oracle  $O_f$  to generate it. Although we can resolve this issue using the specific nature of the problem in some cases such as derivative pricing considered in [27], where the martingale property of the derivative price is used to calculate the function value at one point, it is desirable to devise some generally applicable

\* miyamoto.kouichi.qiqb@osaka-u.ac.jp

† ueda.hiroshi.qiqb@osaka-u.ac.jp

method.

The method proposed in this paper is two-fold. First, we use some *orthogonal function* system. Orthogonal functions such as trigonometric functions, Legendre polynomials, Chebyshev polynomials and so on are the sequences of functions orthogonal to each other with respect to some inner product, which is defined as the weighted integral of the product of two functions over the domain or the sum of the values of the product at the specific nodes. Orthogonal functions are often used for function approximation. That is, any function  $f$  satisfying some conditions on smoothness is approximated as  $f \approx \sum_l a_l P_l$ , the series of orthogonal functions  $\{P_l\}_l$ , with the coefficient  $a_l$  given by the inner product of  $f$  and  $P_l$ . We expect that orthogonal function expansion may be utilized also in the quantum setting, since, as explained later, the coefficient  $a_l$  is given by  $\langle P_l | f \rangle$  times a known factor, with  $|P_l\rangle$  being the quantum state in which  $P_l$  is encoded like  $|f\rangle$ . Thus, by estimating  $\langle P_l | f \rangle$  for every  $l$  up to the sufficiently high order, we get the orthogonal function expansion  $\tilde{f}$  of  $f$ , and then the approximate values of  $f$  at arbitrary points by evaluating  $\tilde{f}$ . This approach seems promising, since we expect that  $\langle P_l | f \rangle$  is not exponentially small, unlike the amplitudes of the computational basis states in  $|f\rangle$ .

However, in the high-dimensional case, the above approach still suffers from the large complexity. If we use the  $D$  orthogonal functions  $\{P_l\}_{l \in [D]_0}$ <sup>1</sup> for accurate approximation in the one-dimensional case, the naive way to achieve the similar accuracy in the  $d$ -dimensional case is using the tensorized functions  $\{P_{l_1, \dots, l_d}\}_{l_1, \dots, l_d \in [D]_0}$ , where  $P_{l_1, \dots, l_d}(x_1, \dots, x_d) = \prod_{i=1}^d P_{l_i}(x_i)$ . In this way, since the total number of  $P_{l_1, \dots, l_d}$ 's is  $D^d$ , obtaining the coefficients  $a_{l_1, \dots, l_d}$  for all  $P_{l_1, \dots, l_d}$ 's and then the orthogonal function expansion of  $f$  takes the exponential complexity, and so does evaluating the resultant expansion. Although the trouble is less serious than reading out the amplitudes in  $|f\rangle$  since we take  $D < n_{\text{gr}}$ , the exponential dependence of the complexity on  $d$  still exists.

Then, we leverage the second building block of our method: *tensor network* (as reviews, see [46, 47]). Tensor network is the approximation scheme for a high-order tensor as a contraction of lower order tensors. In some situations, it approximates the original tensor well, reducing the degrees of freedom (DOF) and the data volume. It was originally invented in quantum many-body physics to approximate wave functions in intractably high-dimensional Hilbert spaces, but nowadays it is utilized in various fields including function approximation [48–54], providing the reduction of the complexity. The recent work [54] shows that the complexity of the tensor network approximation of a  $d$ -dimensional function does not exponentially scale on  $d$  under some condition, which indicates the powerful approximation ability of tensor network.

Another advantage of tensor network is its compatibility with quantum computing. That is, we can generate a quantum state in which a kind of tensor network is amplitude-encoded by a simple quantum circuit [55]. Moreover, there

is a general procedure to optimize such a tensor network circuit so that the fidelity between its resulting state and a given state is maximized [56]. Therefore, we reasonably reach the following idea: given  $O_f$ , we find a tensor network approximation of the coefficients  $a_{l_1, \dots, l_d}$  in the orthogonal function expansion of  $f$  and then an approximate function of  $f$  through the quantum circuit optimization.

In the remaining part of this paper, we show how this idea is realized concretely. We present the tensor network-based quantum circuit and the optimization procedure for making the generated state close to  $|f\rangle$ , based on [56]. The parameters in the tensor network are easily read out from the circuit. To validate our method, we perform the numerical experiment, in which we try to approximate some finance-motivated multivariate function.

This paper is organized as follows. Sec. II describes our method. Beginning with explaining the problem setting under consideration, we present the quantum circuit we use and the procedure to optimize it. In Sec. III, we conduct the aforementioned numerical experiment and see that our method works in this case. Sec. IV summarizes this paper.

## II. OUR METHOD

### A. Problem

As the approximation target, we consider a real-valued function  $f$  on the  $d$ -dimensional hyperrectangle  $\Omega := [L_1, U_1] \times \dots \times [L_d, U_d]$ , where, for  $i \in [d]$ <sup>2</sup>,  $L_i$  and  $U_i$  are real values such that  $L_i < U_i$ .

For any  $i \in [d]$ , we also consider orthogonal functions  $\{P_l^i\}_l$  on  $[L_i, U_i]$  labeled by  $l \in \mathbb{N}_0 := \{0\} \cup \mathbb{N}$ . The orthogonal functions are characterized by the orthogonal relation that, for any  $l, l' \in [D]_0$ ,

$$\int_{L_i}^{U_i} P_l^i(x) P_{l'}^i(x) w^i(x) dx = \delta_{l, l'}, \quad (1)$$

where the weight function  $w^i$  is defined on  $[L_i, U_i]$  and takes the non-negative value, and  $\delta_{l, l'}$  is the Kronecker delta. However, we hereafter assume that  $P_l^i$ 's satisfy the discrete orthogonal relation as follows: for any  $D \in \mathbb{N}$ , there exist  $n_{\text{gr}}$  points  $x_{i,0} < x_{i,1} < \dots < x_{i,n_{\text{gr}}-1}$  in  $[L_i, U_i]$ , where  $n_{\text{gr}} \geq D$ , such that, for any  $l, l' \in [D]_0$ ,

$$\sum_{j=0}^{n_{\text{gr}}-1} P_l^i(x_{i,j}) P_{l'}^i(x_{i,j}) = c_l^i \delta_{l, l'} \quad (2)$$

holds with some  $c_l^i > 0$ . We can consider Eq. (2) as the discrete approximation of Eq. (1), with  $w^i$  absorbed into the spacing of the grid points  $x_{i,j}$ . For some orthogonal functions such as trigonometric functions and Chebyshev polynomials, the relation like Eq. (2) holds even strictly.

<sup>1</sup> For  $n \in \mathbb{N}$ , we define  $[n]_0 := \{0, 1, \dots, n-1\}$ .

<sup>2</sup> For  $n \in \mathbb{N}$ , we define  $[n] := \{1, \dots, n\}$ .

We define the tensorized orthogonal functions as follows: for any  $\vec{l} = (l_1, \dots, l_d) \in \mathbb{N}_0^d$  and  $\vec{x} = (x_1, \dots, x_d) \in \mathbb{R}^d$ ,

$$P_{\vec{l}}(\vec{x}) := \prod_{i=1}^d P_{l_i}^i(x_i). \quad (3)$$

It follows from Eq. (2) that, with  $\vec{x}_{\vec{j}}$  defined as  $\vec{x}_{\vec{j}} := (x_{1,j_1}, \dots, x_{d,j_d}) \in \mathbb{R}^d$  for any  $\vec{j} = (j_1, \dots, j_d) \in [n_{\text{gr}}]_0^d$ , they satisfy the orthogonal relation

$$\sum_{\vec{j} \in [n_{\text{gr}}]_0^d} P_{\vec{l}}(\vec{x}_{\vec{j}}) P_{\vec{l}'}(\vec{x}_{\vec{j}}) = c_{\vec{l}} \delta_{\vec{l}, \vec{l}'} \quad (4)$$

for any  $\vec{l} = (l_1, \dots, l_d)$  and  $\vec{l}' = (l'_1, \dots, l'_d)$  in  $[D]_0^d$ , where  $\delta_{\vec{l}, \vec{l}'} := \prod_{i=1}^d \delta_{l_i, l'_i}$  and  $c_{\vec{l}} := \prod_{i=1}^d c_{l_i}$ .

Then, our goal is to find an approximation  $\tilde{f}$  of  $f$  in the form of

$$\tilde{f}(\vec{x}) = \sum_{\vec{l} \in [D]_0^d} a_{\vec{l}} P_{\vec{l}}(\vec{x}) \quad (5)$$

with  $D$  set sufficiently large. Here, for any  $\vec{l} \in [D]_0^d$ , the coefficient  $a_{\vec{l}}$  is given by

$$a_{\vec{l}} = \frac{1}{c_{\vec{l}}} \sum_{\vec{j} \in [n_{\text{gr}}]_0^d} f(\vec{x}_{\vec{j}}) P_{\vec{l}}(\vec{x}_{\vec{j}}), \quad (6)$$

which follows from Eq. (2). It is known that this kind of series converges to  $f$  in the large  $D$  limit for some orthogonal functions (see [57] for the trigonometric series and [58] for the Chebyshev series).

## B. Oracles to generate the function-encoding states

In this paper, we assume the availability of the oracle  $O_f$  explained in the introduction. We now define it strictly. We hereafter assume that the grid number  $n_{\text{gr}}$  satisfies  $n_{\text{gr}} = 2^{m_{\text{gr}}}$  with some integer  $m_{\text{gr}}$ . Then, we consider the system  $S$  consisting of  $d$   $m_{\text{gr}}$ -qubit registers and the unitary operator  $O_f$  that acts on  $S$  as

$$O_f |0\rangle^{\otimes d} = |f\rangle := \frac{1}{C} \sum_{\vec{j}=(j_1, \dots, j_d) \in [n_{\text{gr}}]_0^d} f(\vec{x}_{\vec{j}}) |j_1\rangle \cdots |j_d\rangle. \quad (7)$$

Here and hereafter, for any  $n \in \mathbb{N}_0$ , we denote by  $|n\rangle$  the computational basis states on the quantum register with the sufficient number of qubits, in which the bit string on the register corresponds to the binary representation of  $n$ .  $|j\rangle$  with  $j \in [n_{\text{gr}}]_0$  in Eq. (7) is the computational basis state on a  $m_{\text{gr}}$ -qubit register. Besides,  $C$  in Eq. (7) is defined as

$$C := \sqrt{\sum_{j \in [n_{\text{gr}}]_0^d} (f(\vec{x}_{\vec{j}}))^2}. \quad (8)$$

We also assume that the availability of the oracles  $V_{\text{OF}}^1, \dots, V_{\text{OF}}^d$ , each of which acts on a  $m_{\text{gr}}$ -qubit register as

$$V_{\text{OF}}^i |l\rangle = |P_l^i\rangle := \frac{1}{\sqrt{c_l^i}} \sum_{j=0}^{n_{\text{gr}}-1} P_l^i(x_{i,j}) |j\rangle \quad (9)$$

for any  $l \in [D]_0$ .  $V_{\text{OF}}^i |D\rangle, \dots, V_{\text{OF}}^i |n_{\text{gr}} - 1\rangle$  may be any states as far as  $V_{\text{OF}}^i$  is unitary. These oracles are in principle constructible because of the orthogonal relation (2). The more concrete implementation of them is discussed in Appendix A. Note that, for any  $\vec{l} \in [D]_0^d$ , we have

$$\langle P_{\vec{l}}^i | f \rangle = \frac{1}{C \sqrt{c_{\vec{l}}^i}} \sum_{\vec{j} \in [n_{\text{gr}}]_0^d} f(\vec{x}_{\vec{j}}) P_{\vec{l}}^i(\vec{x}_{\vec{j}}) = \frac{\sqrt{c_{\vec{l}}^i}}{C} a_{\vec{l}}, \quad (10)$$

where  $|P_{\vec{l}}^i\rangle := |P_{l_1}^i\rangle \cdots |P_{l_d}^i\rangle$ . Since both  $C$  and  $\sqrt{c_{\vec{l}}^i}$  are the root mean squares of some functions over the grid points, we expect that their ratio is  $O(1)$  and that we can efficiently obtain  $a_{\vec{l}}$  through estimating  $\langle P_{\vec{l}}^i | f \rangle$ . However, we do not consider this direction in this paper, since finding all the expansion coefficients suffers from the exponential increase of the coefficient number in the high-dimensional case, as explained in the introduction.

## C. Matrix product state

Thus, we hereafter consider to use tensor network. Among various kinds of tensor network, we use the *matrix product state (MPS)*, also known as the *tensor train*, which is simple but powerful and so widely used in various fields. In the

scheme of MPS, the order- $d$  tensor  $a_{\vec{l}} \in \mathbb{R}^{\overbrace{D \times \cdots \times D}^d}$  is approximated by

$$\tilde{a}_{\vec{l}} := \sum_{k_1=1}^r \cdots \sum_{k_{d-2}=1}^r U_{l_1, k_1}^1 U_{k_1, l_2, k_2}^2 \cdots U_{k_{d-3}, l_{d-2}, k_{d-2}}^{d-2} U_{k_{d-2}, l_{d-1}, l_d}^{d-1}, \quad (11)$$

where  $r \in \mathbb{N}$  is called the bond dimension,  $U^1 \in \mathbb{R}^{D \times r}$ ,  $U^i \in \mathbb{R}^{r \times D \times r}$  for  $i \in \{2, \dots, d-2\}$ , and  $U^{d-1} \in \mathbb{R}^{r \times D \times D}$ .<sup>3</sup>

<sup>3</sup> Usually, the MPS representation of a  $d$ -dimensional tensor is in the form of

$$\tilde{a}_{\vec{l}} := \sum_{k_1=1}^r \cdots \sum_{k_{d-1}=1}^r U_{l_1, k_1}^1 U_{k_1, l_2, k_2}^2 \cdots U_{k_{d-2}, l_{d-1}, k_{d-1}}^{d-1} U_{k_{d-1}, l_d}^d, \quad (12)$$

where, in comparison to Eq. (11),  $(U_{k_{d-2}, l_{d-1}, k_{d-1}}^{d-1})$  is in not  $\mathbb{R}^{r \times D \times D}$  but  $\mathbb{R}^{r \times D \times r}$ , and  $(U_{k_{d-1}, l_d}^d) \in \mathbb{R}^{r \times D}$  is added. We can consider that  $U^{d-1}$  and  $U^d$  in Eq. (12) is contracted to  $U^{d-1}$  in Eq. (11). The reason of the form in Eq. (11) is that it corresponds to the quantum circuit considered in Sec. IID. Besides, although we can set the bond dimension  $r$  separately for each pair of  $U^i$  and  $U^{i+1}$ , we set it to the same value for simplicity in this paper.

Note that there are many ways of decomposition like the RHS of Eq. (11) that gives the same tensor  $\tilde{a}_\gamma$ . For example, if we can decompose  $U^i$  as

$$U_{k_{i-1}, l_i, k_i}^i = \sum_{k'=1}^r R_{k_{i-1}, k'} \tilde{U}_{k', l_i, k_i}^i \quad (13)$$

with some  $R \in \mathbb{R}^{r \times r}$  and  $\tilde{U}^i \in \mathbb{R}^{r \times D \times r}$ , replacing  $U_{k_{i-2}, l_{i-1}, k_{i-1}}^{i-1}$  and  $U_{k_{i-1}, l_i, k_i}^i$  in Eq. (11) with  $\sum_{k'=1}^r U_{k_{i-2}, l_{i-1}, k'}^{i-1} R_{k', k_{i-1}}$  and  $\tilde{U}_{k_{i-1}, l_i, k_i}^i$ , respectively, does not change  $a_\gamma$ . Therefore, we hereafter assume the following conditions: for any  $i \in \{2, \dots, d-2\}$  and  $k_{i-1}, k'_{i-1} \in [r]$ ,

$$\sum_{l_i=0}^{D-1} \sum_{k_i=1}^r U_{k_{i-1}, l_i, k_i}^i U_{k'_{i-1}, l_i, k_i}^i = \delta_{k_{i-1}, k'_{i-1}} \quad (14)$$

$$\tilde{f}(\vec{x}) = \sum_{\vec{l} \in [D]_0^d} \tilde{a}_\gamma P_{\vec{l}}(\vec{x}) = \sum_{l_1=0}^{D-1} \cdots \sum_{l_d=0}^{D-1} \sum_{k_1=1}^r \cdots \sum_{k_{d-2}=1}^r U_{l_1, k_1}^1 U_{k_1, l_2, k_2}^2 \cdots U_{k_{d-3}, l_{d-2}, k_{d-2}}^{d-2} U_{k_{d-2}, l_{d-1}, l_d}^{d-1} P_{l_1}^1(x_1) \cdots P_{l_d}^d(x_d). \quad (17)$$

This can be computed as

$$\tilde{f}(\vec{x}) = \sum_{k_1=1}^r \cdots \sum_{k_{d-2}=1}^r \left( \sum_{l_1=0}^{D-1} U_{l_1, k_1}^1 P_{l_1}^1(x_1) \right) \times \left( \sum_{l_2=0}^{D-1} U_{k_1, l_2, k_2}^2 P_{l_2}^2(x_2) \right) \times \cdots \times \left( \sum_{l_{d-2}=0}^{D-1} U_{k_{d-3}, l_{d-2}, k_{d-2}}^{d-2} P_{l_{d-2}}^{d-2}(x_{d-2}) \right) \times \left( \sum_{l_{d-1}, l_d=0}^{D-1} U_{k_{d-2}, l_{d-1}, l_d}^{d-1} P_{l_{d-1}}^{d-1}(x_{d-1}) P_{l_d}^d(x_d) \right), \quad (18)$$

that is, we first contract  $U_{k_{i-1}, l_i, k_i}^i$  and  $P_{l_i}^i$  with respect to  $l_i$  for each  $i \in [d]$ , and then take contractions with respect to  $k_1, \dots, k_{d-2}$ . In this procedure, the number of arithmetic operations is

$$O(dr^2D + rD^2), \quad (19)$$

which is much smaller than  $O(D^d)$  for computing (5) with general  $a_\gamma$  not having any specific structure.

#### D. Quantum circuit to generate the tensor network state

The quantum circuit to generate a MPS-encoded quantum state is shown in Fig. 1. First, we prepare  $dm_{\text{deg}}$  qubits initial-

$$V_{\text{MPS}} |0\rangle^{\otimes d} = |\tilde{a}\rangle := \sum_{l_1=0}^{D-1} \cdots \sum_{l_d=0}^{D-1} \sum_{k_1=1}^r \cdots \sum_{k_{d-2}=1}^r U_{l_1, k_1}^1 U_{k_1, l_2, k_2}^2 \cdots U_{k_{d-3}, l_{d-2}, k_{d-2}}^{d-2} U_{k_{d-2}, l_{d-1}, l_d}^{d-1} |l_1\rangle \cdots |l_d\rangle. \quad (20)$$

In Eq. (20),  $|l\rangle$  with  $l \in [D]_0$  denotes the computational basis states on  $S_{\text{deg},1}, \dots, S_{\text{deg},d}$ . Besides, we have associated the

holds, and, for any  $k_{d-2}, k'_{d-2} \in [r]$ ,

$$\sum_{l_{d-1}=0}^{D-1} \sum_{l_d=0}^{D-1} U_{k_{d-2}, l_{d-1}, l_d}^{d-1} U_{k'_{d-2}, l_{d-1}, l_d}^{d-1} = \delta_{k_{d-2}, k'_{d-2}} \quad (15)$$

holds. These can be always satisfied by QR decomposition of  $U^i$ 's and redefinition [59].

Also note that the representation like Eq. (11) actually reduces the DOF compared with the original  $a_\gamma$  as a  $d$ -dimensional tensor. The total number of the components in  $U^1, \dots, U^{d-1}$  is

$$rD + (d-3)r^2D + rD^2, \quad (16)$$

which is smaller than that in  $a_\gamma$ ,  $D^d$ , unless we take  $r = O(D^{O(d)})$ . Besides, with the coefficients  $a_\gamma$  in Eq. (5) represented as Eq. (11), the computation of the approximation of the function  $f$  becomes efficient in fact. We now approximate  $f$  by

ized to  $|0\rangle$ , where we assume that  $D = 2^{m_{\text{deg}}}$  holds with some  $m_{\text{deg}} \in \mathbb{N}$ . Labeling them by the integers  $1, \dots, dm_{\text{deg}}$ , for each  $i \in [d]$ , we denote the system of the  $((i-1)m_{\text{deg}}+1)$ th to  $im_{\text{deg}}$ th qubits by  $S_{\text{deg},i}$ . Besides, assuming that  $r = 2^{m_{\text{BD}}}$  also holds with some  $m_{\text{BD}} \in \mathbb{N}$ , for each  $i \in [d-2]$ , we denote the system of  $S_{\text{deg},i}$  and the first  $m_{\text{BD}}$  qubits in  $S_{\text{deg},i+1}$  by  $S'_{\text{deg},i}$ , and the system of the last  $2m_{\text{deg}}$  qubits by  $S'_{\text{deg},d-1}$ . Then, we put the quantum gates  $V_1, \dots, V_{d-1}$  on  $S'_{\text{deg},1}, \dots, S'_{\text{deg},d-1}$ , respectively, in this order.

Let us denote by  $V_{\text{MPS}}$  the unitary that corresponds to the whole of the above quantum circuit. Then,  $V_{\text{MPS}}$  actually generates the MPS-encoded state

entries in  $U^1, \dots, U^{d-1}$  with those in  $V^1, \dots, V^{d-1}$  as unitaries,

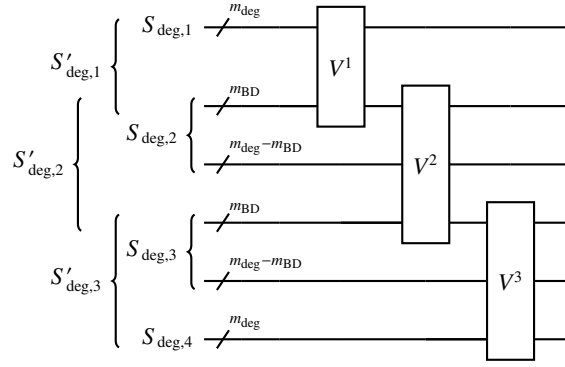


FIG. 1: The quantum circuit  $V_{\text{MPS}}$  that generates the MPS-encoded state (20) in the case of  $d = 4$ . All the  $dm_{\text{deg}}$  qubits are initialized to  $|0\rangle$ . The subsystems consisting of a part of the qubits, which are indicated in the left end, are as described in the body text.

respectively, as follows:

$$U_{l_1, k_1}^1 = \langle l_1 + Dk_1 | V^1 | 0 \rangle \quad (21)$$

for any  $l_1 \in [D]_0$  and  $k_1 \in [r]$ ,

$$U_{k_{i-1}, l_i, k_i}^i = \langle l_i + Dk_i | V^i | k_{i-1} \rangle \quad (22)$$

for any  $i \in \{2, \dots, d-2\}$ ,  $l_i \in [D]_0$  and  $k_{i-1}, k_i \in [r]$ , and

$$U_{k_{d-2}, l_{d-1}, l_d}^{d-1} = \langle l_{d-1} + Dl_d | V^{d-1} | k_{d-2} \rangle \quad (23)$$

for any  $l_{d-1}, l_d \in [D]_0$  and  $k_{d-2} \in [r]$ , where  $|n\rangle$  with  $n \in \mathbb{N}_0$  denotes the computational basis state on either of  $S'_{\text{deg},1}, \dots, S'_{\text{deg},d-1}$ . Although  $V^1, \dots, V^{d-1}$  have the other components than those that appear in Eqs. (21) to (23), they do not affect the state  $|\tilde{a}\rangle$  because of the initialization of all the qubits to  $|0\rangle$ .

Note that  $U^2, \dots, U^{d-1}$  in Eqs. (22) and (23) automatically satisfy the conditions (14) and (15) because of the unitarity of  $V^2, \dots, V^{d-1}$ . On the other hand, the unitarity of  $V^1$  imposes the constraint

$$\sum_{l_1=0}^{D-1} \sum_{k_1=1}^r |U_{l_1, k_1}^1|^2 = 1 \quad (24)$$

$$V_{\text{App}} |0\rangle^{\otimes d} = |\tilde{f}\rangle := \sum_{l_1=0}^{D-1} \cdots \sum_{l_d=0}^{D-1} \sum_{k_1=1}^r \cdots \sum_{k_{d-2}=1}^r \sum_{j_1=0}^{n_{\text{gr}}-1} \cdots \sum_{j_d=0}^{n_{\text{gr}}-1} U_{l_1, k_1}^1 U_{k_1, l_2, k_2}^2 \cdots U_{k_{d-3}, l_{d-2}, k_{d-2}}^{d-2} U_{k_{d-2}, l_{d-1}, l_d}^{d-1} P_{l_1}^1(x_{1, j_1}) \cdots P_{l_d}^d(x_{d, j_d}) |j_1\rangle \cdots |j_d\rangle, \quad (25)$$

where  $|n\rangle$  with  $n \in \mathbb{N}_0$  now denotes the computational basis state on  $S_{\text{gr},1}, \dots, S_{\text{gr},d}$ . That is, this is the quantum state that amplitude-encodes  $\tilde{f}$  in Eq. (17), the approximation of  $f$  by the orthogonal function expansion and the MPS approximation of the coefficients. Therefore, if we obtain  $V_{\text{App}}$  that generates  $|\tilde{f}\rangle$  close to  $|f\rangle$ , we also obtain  $\{U^i\}_i$  for which  $\tilde{f}$  in Eq.

on  $U^1$  in Eq. (21). This means the following: with such  $U^1$ , the MPS-based approximation  $\tilde{f}$  in Eq. (17) does not have the DOF of the overall factor, and therefore, although we can express the functional form of  $f$  by  $\tilde{f}$ , we cannot adjust the magnitude of  $\tilde{f}$  so that it fits  $f$ . Conversely, if we have some estimate  $C$  for the ratio of  $f$  to  $\tilde{f}$ , we can approximate  $f$  by  $C\tilde{f}$ . This issue will be addressed in Section II E.

## E. Optimization of the quantum circuit

We now consider how to optimize the quantum circuit  $V_{\text{MPS}}$  and obtain the MPS-based function approximation.

We first extend the circuit  $V_{\text{MPS}}$  in Section II D using  $\{V_{\text{OF}}^i\}_i$  as follows. For each  $i \in [d]$ , we add  $m_{\text{gr}} - m_{\text{deg}}$  qubits after the  $i$ th qubits in the original circuit, and denote the system consisting of  $S_{\text{deg},i}$  and the added qubits by  $S_{\text{gr},i}$ . Note that the resultant system is same as the system  $S$  for  $O_f$ , which consists of the  $d$   $m_{\text{gr}}$ -qubit registers. We then perform  $V_{\text{OF}}^i$  on  $S_{\text{deg},i}$ . The resultant circuit  $V_{\text{App}}$  is shown in Fig. 2. Note that this circuit generates

(17) well approximate  $f$  at least on the grid points, by reading out their entries from the quantum gates  $\{V^i\}_i$  in  $V_{\text{App}}$ , except the overall factor  $C$ .

We next consider how to obtain such  $V_{\text{App}}$ , especially  $\{V^i\}_i$  in it. We aim at maximizing the fidelity

$$F = \langle f | \tilde{f} \rangle. \quad (26)$$

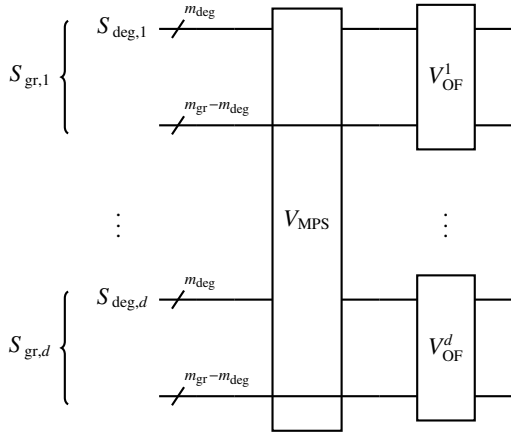


FIG. 2: The quantum circuit  $V_{\text{App}}$  that generates the state (25) in which the approximation  $\tilde{f}$  in Eq. (17) of  $f$  is amplitude-encoded. The circuit  $V_{\text{MPS}}$  is that in Fig. 1, where the lines going over this means that they are not used in it. All the  $dm_{\text{gr}}$  qubits are initialized to  $|0\rangle$ . The subsystems consisting of a part of the qubits, which are indicated in the left end, are as described in the body text.

Note that maximizing  $F$  is equivalent to minimizing the sum of the squared difference between the two normalized functions

$$\sum_{\vec{j} \in [n_{\text{gr}}]_0^d} \left( \frac{f(\vec{x}_{\vec{j}})}{C} - \tilde{f}(\vec{x}_{\vec{j}}) \right)^2, \quad (27)$$

which is, in the large  $n_{\text{gr}}$  limit, equivalent to

$$\int_{\Omega} \left( \frac{f(\vec{x}_{\vec{j}})}{C} - \tilde{f}(\vec{x}_{\vec{j}}) \right)^2 w^1(x_1) \cdots w^d(x_d) d\vec{x}, \quad (28)$$

that is, the squared  $L^2$  norm of  $\frac{f}{C} - \tilde{f}$ , the common metric in function approximation.

The procedure of maximizing  $F$  is similar to that presented in [56]. We try to optimize each of  $\{V^i\}$  alternately. That is, we optimize  $V^i$  with the others fixed, setting  $i$  to 1, 2, ...,  $d-1$  in turn. We may repeat this loop for the arbitrary times. In the step to optimize  $V^i$ , it is updated as follows. We define

$$F_i = \text{Tr}_{S'_{\text{deg},i}} [|\Psi_{i+1}\rangle \langle \Phi_{i-1}|]. \quad (29)$$

Here,  $\bar{S}'_{\text{deg},i}$  denote the system consisting of the qubits except those in  $S'_{\text{deg},i}$ , and, for any subsystem  $s$  in  $S$ ,  $\text{Tr}_s$  means the partial trace over the Hilbert space corresponding to  $s$ .  $|\Psi_{i+1}\rangle$  is defined as

$$|\Psi_{i+1}\rangle = \begin{cases} \left( (V^{i+1} \otimes I_{\bar{S}'_{\text{deg},i+1}})^\dagger \cdots (V^{d-1} \otimes I_{\bar{S}'_{\text{deg},d-1}})^\dagger (V_{\text{OF}}^1 \otimes \cdots \otimes V_{\text{OF}}^{d-1})^\dagger |f\rangle \right) & ; \text{ for } i = 1, \dots, d-2 \\ (V_{\text{OF}}^1 \otimes \cdots \otimes V_{\text{OF}}^{d-1})^\dagger |f\rangle & ; \text{ for } i = d-1 \end{cases} \quad (30)$$

where  $I_{\bar{S}'_{\text{deg},i}}$  denotes the identity operator on  $\bar{S}'_{\text{deg},i}$ , and thus  $V^i \otimes I_{\bar{S}'_{\text{deg},i}}$  simply denotes the  $i$ th block in  $V_{\text{MPS}}$  in Fig. 1.  $|\Phi_{i-1}\rangle$  is defined as

$$|\Phi_{i-1}\rangle = \begin{cases} \left( (V^{i-1} \otimes I_{\bar{S}'_{\text{deg},i-1}}) \cdots (V^1 \otimes I_{\bar{S}'_{\text{deg},1}}) |0\rangle^{\otimes d} \right) & ; \text{ for } i = 2, \dots, d-1 \\ |0\rangle^{\otimes d} & ; \text{ for } i = 1 \end{cases} \quad (31)$$

We can regard this  $F_i$  as the  $M \times M$  matrix, where  $M = rD$  for  $i \in [d-2]$  and  $M = D^2$  for  $i = d-1$ . Its entries are given by  $\langle l|F_i|l'\rangle$ , where  $|l\rangle, |l'\rangle \in \{|0\rangle, |1\rangle, \dots, |M-1\rangle\}$  are now the computational basis states on  $S'_{\text{deg},i}$ . Supposing that we know  $F_i$ , we perform its singular value decomposition (SVD)

$$F_i = XDY, \quad (32)$$

where  $X$  and  $Y$  are the  $M \times M$  unitaries and  $D$  is the diagonal matrix having the singular values of  $F_i$  as its diagonal entries. We finally update  $V^i$  by

$$V^i = XY. \quad (33)$$

We obtain  $F_i$  through the Pauli decomposition and the Hadamard test [56]. We set  $m = \log_2 M$ , and, for any  $k \in [m]$ , we denote the identity operator, the Pauli-X gate, the Pauli-Y gate and the Pauli-Z gate on the  $k$ th qubit in  $S'_{\text{deg},i}$  by  $\hat{\sigma}_0^k, \hat{\sigma}_1^k, \hat{\sigma}_2^k$  and  $\hat{\sigma}_3^k$ , respectively. We also define

$$\hat{\sigma}_{\vec{\alpha}} := \hat{\sigma}_{\alpha_1}^1 \otimes \cdots \otimes \hat{\sigma}_{\alpha_m}^m \quad (34)$$

for any  $\vec{\alpha} = (\alpha_1, \dots, \alpha_m) \in \{0, 1, 2, 3\}^m$ . Then, we can always decompose  $F_i$  as

$$F_i = \sum_{\vec{\alpha} \in \{0,1,2,3\}^{m'}} \tilde{F}_{i,\vec{\alpha}} \hat{\sigma}_{\vec{\alpha}} \quad (35)$$

with  $\tilde{F}_{i,\vec{\alpha}} \in \mathbb{C}$ . Since

$$\text{Tr}_{S'_{\text{deg},i}} [F_i \hat{\sigma}_{\vec{\alpha}}] = M \tilde{F}_{i,\vec{\alpha}} \quad (36)$$

holds, we obtain  $\tilde{F}_{i,\vec{\alpha}}$  through estimation of  $\text{Tr}_{S'_{\text{deg},i}} [F_i \hat{\sigma}_{\vec{\alpha}}]$ . Noting that

$$\text{Tr}_{S'_{\text{deg},i}} [F_i \hat{\sigma}_{\vec{\alpha}}] = \langle \Phi_{i-1} | \hat{\sigma}_{\vec{\alpha}} | \Psi_{i+1} \rangle, \quad (37)$$

we can estimate this by the Hadamard test, in which the circuit  $V_{\text{MPS}}$  with replacement of  $V^i$  with  $\hat{\sigma}_{\vec{\alpha}}$  is used. We refer to [56] for its details.

After we optimize  $\{V^i\}$  and read out  $\{U^i\}$  from them, the remaining task is just multiplying the factor  $C$  to  $\tilde{f}$  constructed from  $\{U^i\}$ . In this paper, we do not go into the details of estimating this factor but simply assume that we have some estimate of it. In fact, in some quantum algorithm for PDE solving, the way to estimate this factor, the root of the squared sum of the function values on the grid points, is presented [19].

Now, let us summarize the whole procedure to obtain an approximation of  $f$  as Algorithm 1.

---

**Algorithm 1** The proposed algorithm to obtain an approximation of the function  $f : \Omega \rightarrow \mathbb{R}$ .

---

**Input:**

- 1:
    - $D = 2^{m_{\text{deg}}}$  with  $m_{\text{deg}} \in \mathbb{N}$ : the degree of the orthogonal functions
    - $r = 2^{m_{\text{BD}}}$  with  $m_{\text{BD}} \in \mathbb{N}$ : the bond dimension
    - The oracle  $O_f$  in Eq. (7).
    - The orthogonal functions  $\{P_l^i\}_{i \in [d], l \in [D]_0}$  satisfying Eq. (2).
    - The iteration  $n_{\text{iter}} \in \mathbb{N}$  of the optimization loop.
    - The initial values of the  $rD \times rD$  unitaries  $V^1, \dots, V^{d-2}$  and the  $D^2 \times D^2$  unitary  $V^{d-1}$ , which may be chosen randomly.
    - The estimate  $\tilde{C}$  of  $C$  in Eq. (8).
  - 2: **for**  $i_{\text{iter}} = 1$  to  $n_{\text{iter}}$  **do**
  - 3:   **for**  $i = 1$  to  $d - 1$  **do**
  - 4:     **for**  $\vec{\alpha} \in \{0, 1, 2, 3\}^m$  **do**
  - 5:       Estimate  $\langle \Phi_{i-1} | \hat{\sigma}_{\vec{\alpha}} | \Psi_{i+1} \rangle$  by the Hadamard test, and let it divided by  $M$  be  $\tilde{F}_{\vec{\alpha}}$ .
  - 6:       **end for**
  - 7:       Set  $F_i$  as Eq. (35).
  - 8:       Perform the SVD of  $F_i$  as Eq. (32).
  - 9:       Update  $V^i$  as Eq. (33).
  - 10:     **end for**
  - 11: **end for**
  - 12: Set  $U^1 \in \mathbb{R}^{D \times r}$ ,  $U^i \in \mathbb{R}^{r \times D \times r}$  for  $i \in \{2, \dots, d-2\}$ , and  $U^{d-1} \in \mathbb{R}^{r \times D \times D}$  as Eqs. (21), (22) and (23), respectively.
  - 13: Define  $\tilde{f}$  as Eq. (17).
  - 14: Output  $\tilde{C}\tilde{f}$  as an approximation of  $f$ .
- 

### III. NUMERICAL EXPERIMENT

Now, we confirm the feasibility of our method by the numerical experiment on approximating a finance-motivated function.

#### A. Approximated function

As a reasonable instance for the target function of the approximation, we take the price of some financial derivative.

A *financial derivative*, or simply a *derivative*, is a contract between two parties in which the amounts (the *payoffs*) determined by the prices of some widely traded assets (*underlying assets*) such as stocks and bonds are paid and/or received between the parties. Under some mathematical model that describes the random movement of the underlying asset prices, we can use the established theory to calculate the derivative price (see [60, 61] as the famous textbooks).

Here, we consider the  $d$  underlying assets whose prices  $\vec{S}(t) = (S_1(t), \dots, S_d(t))$  at time  $t$  obey the Black-Scholes (BS) model [62, 63] characterized by the following stochastic differential equation (SDE) in the risk-neutral measure: for  $i \in [d]$ ,

$$dS_i(t) = r_{\text{RF}}S_i(t)dt + \sigma_i S_i(t)dW_i(t). \quad (38)$$

Here,  $r_{\text{RF}}$  is the real parameter called the risk-free interest rate and  $\sigma_1, \dots, \sigma_d$  are the positive parameters called the volatilities.  $W_1, \dots, W_d$  are the Brownian motions and satisfies  $dW_i dW_j = \rho_{ij} dt$  for  $i, j \in [d]$ , where the correlation matrix  $(\rho_{ij})$  is symmetric and positive definite and satisfies  $\rho_{11} = \dots = \rho_{dd} = 1$  and  $-1 < \rho_{ij} < 1$  if  $i \neq j$ .  $t = 0$  corresponds to the present.

We also consider the derivative in which one party A receives the payoff from the other party B at the predetermined time  $T > 0$  and its amount  $f_{\text{pay}}(\vec{S}(T))$  depends on the underlying asset prices at  $T$ . Under some technical assumptions, the price of this derivative for A at time  $t \in [0, T)$  with  $\vec{S}(t)$  being  $\vec{s} = (s_1, \dots, s_d)$  is given by

$$V(t, \vec{s}) = E \left[ e^{-r_{\text{RF}}(T-t)} f_{\text{pay}}(\vec{S}(T)) \mid \vec{S}(t) = \vec{s} \right], \quad (39)$$

where  $E[\cdot]$  denotes the (conditional) expectation in the risk-neutral measure. This expectation can be calculated by Monte Carlo integration, that is, generating many sample paths of the time evolution of  $\vec{S}(t)$  up to  $T$  and averaging  $e^{-r_{\text{RF}}(T-t)} f_{\text{pay}}(\vec{S}(T))$  on the paths. It is also known that we find  $V(t, \vec{s})$  by solving the BS PDE

$$\begin{aligned} \frac{\partial}{\partial t} V(t, \vec{s}) + \frac{1}{2} \sum_{i,j=1}^d \sigma_i \sigma_j \rho_{ij} s_i s_j \frac{\partial^2}{\partial s_i \partial s_j} V(t, \vec{s}) \\ + r_{\text{RF}} \left( \sum_{i=1}^d s_i \frac{\partial}{\partial s_i} V(t, \vec{s}) - V(t, \vec{s}) \right) = 0 \end{aligned} \quad (40)$$

backward from time  $T$  to  $t$ , with the boundary condition in the time direction being

$$V(T, \vec{s}) = f_{\text{pay}}(\vec{s}) \quad (41)$$

and those in  $\vec{s}$  directions set according to the asymptotic behavior of  $V(t, \vec{s})$  in the small and large asset price limit. In fact, solving the BS PDE by quantum computing has been considered in some previous works [27, 32, 36–38].

For concreteness, we hereafter consider the *worst-of-put* option, which has the payoff function

$$f_{\text{pay}}(\vec{s}) = \max\{K - \min\{s_1, \dots, s_d\}, 0\}, \quad (42)$$

and is often incorporated in exotic equity derivatives. Here,  $K$  is a positive constant called the strike.

Hereafter, we try to approximate  $V(0, \vec{s})$  as a function of  $\vec{s}$ . Since we cannot evaluate this analytically, we compute its values on the grid points, which are explicitly given later, by Monte Carlo integration with  $10^5$  sample paths, and use them in the following part of the experiment. In this calculation, we have used TF Quant Finance library [64].

#### B. Orthogonal functions

We use cosine functions as orthogonal functions. Concretely, for any  $i \in [d]$  and  $l \in [D]_0$ , we set

$$P_l^i(x_i) = \cos \left( l \frac{x_i - L_i}{U_i - L_i} \pi \right) \quad (43)$$

where  $U_i$  is set by

$$U_i = K \exp\left(\sqrt{2\sigma_i^2 T} \log \frac{dK}{\epsilon}\right) \quad (44)$$

with  $\epsilon = 0.01$ , following the study [65] on the appropriate grid setting for solving the BS PDE, and  $L_i = 0.01K$ . The orthogonal relation (2) is satisfied with the grid points set as

$$x_{i,j} = \frac{j + \frac{1}{2}}{n_{\text{gr}}}(U_i - L_i) + L_i \quad (45)$$

for  $j \in [n_{\text{gr}}]_0$  and  $c_l^j$  being

$$c_l^j = \begin{cases} n_{\text{gr}} & ; \text{ for } l = 0 \\ \frac{n_{\text{gr}}}{2} & ; \text{ for } l \in [D - 1] \end{cases}. \quad (46)$$

### C. Modifications on the algorithm to run the numerical experiment

We use Algorithm 1 but made the following modification, since we do all calculations on a classical computer, and thus there is the memory space limitation. We try to maximize not  $F$  in Eq. (26) but

$$F' = \langle a | \tilde{a} \rangle \quad (47)$$

Here,  $|\tilde{a}\rangle$  is given in Eq. (20) and

$$|a\rangle := \sqrt{\frac{1}{\sum_{\vec{l} \in [D]_0^d} |a_{\vec{l}}|^2}} \sum_{\vec{l} \in [D]_0^d} a_{\vec{l}} |l_1\rangle \cdots |l_d\rangle, \quad (48)$$

where we calculate the coefficients  $a_{\vec{l}}$  for each  $\vec{l} \in [D]_0^d$  by Eq. (6), using the values of  $V(0, \vec{s})$  on the grid points computed by Monte Carlo integration as  $f(\vec{x}_{\vec{l}})$ . We take the minimal grid points to calculate the coefficients for given  $D$ , which means  $n_{\text{gr}} = D$ , although it is supposed that  $n_{\text{gr}} > D$  when our algorithm is used on the future quantum computer with the oracle  $O_f$ .

By this modification, the quantum circuit under consideration becomes small and the calculation becomes feasible on a classical computer. The gates  $\{V_{\text{OF}}^i\}$  do not appear in our experiment, with their roles absorbed into the aforementioned preprocessing to calculate  $\{a_{\vec{l}}\}$ . Besides, most importantly, note that  $\{U^i\}$  calculated under the above modification is same as those output by our algorithm without the modification.

### D. Result of the approximation

We then try to get the approximation of  $V(0, \vec{s})$ . We set the parameters as follows:  $d = 5, D = r = 16, n_{\text{iter}} = 5, r_{\text{RF}} = 0, \sigma_1 = \dots = \sigma_5 = 0.2, K = 100, T = 1$ . For the estimation  $\tilde{C}$  of  $C$ , we use the root squared sum of the values of  $V(0, \vec{s})$  on the grid points, which are calculated by Monte Carlo integration as mentioned in Sec. III A. We use ITensor library [66] for tensor calculation.

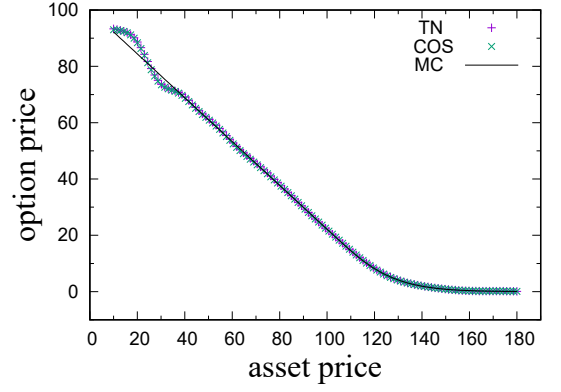


FIG. 3: The five-asset worst-of put option prices  $V(0, \vec{s})$  for  $s_1 = \dots = s_5 = s$  calculated in the various ways. The horizontal and vertical axes correspond to  $s$  and  $V(0, \vec{s})$ , respectively. The +,  $\times$ , and black line indicate those by the MPS-based approximation, the cosine expansion approximation and Monte Carlo integration, respectively.

We display the obtained MPS-based approximation of  $V(0, \vec{s})$  in Fig. 3 along with the Monte Carlo integration values and the cosine expansion approximation as Eq. (5). Since it is difficult to plot the function value over the high-dimensional space, we only show the values on the “diagonal” line  $s_1 = \dots = s_d$ . The figure shows that the MPS-based approximation well fits the Monte Carlo integration values except the region near the lower end of the domain of the approximations. Note that the cosine expansion approximation already has the error from the Monte Carlo values, and the MPS-based approximation never has the better error than it. We see that the MPS-based approximation almost overlaps the cosine expansion approximation, which means that the MPS-based approximation is working well.

In the current MPS-based approximation, the number of the DOF is 12544, which is smaller than the number of the cosine expansion coefficients 1048576 by two orders of magnitude. Therefore, we have achieved the large parameter reduction keeping the approximation accuracy.

### E. Relationship between the approximation accuracy and the degrees of freedom

In order to investigate the relationship between the DOF and the approximation accuracy, we perform the following additional experiment. We replace the circuit  $V_{\text{MPS}}$  in Fig. 1 with the different one  $V'_{\text{MPS}}$  having the different DOF. Here, with  $m_{\text{bl}} \in \{2, \dots, dm_{\text{deg}} - 1\}$ ,  $V'_{\text{MPS}}$  consists of the gates  $\tilde{V}^1, \dots, \tilde{V}^{dm_{\text{deg}} - m_{\text{bl}} + 1}$  that act on the systems of  $m_{\text{bl}}$  qubits displaced one by one, as shown in Fig. 4. The DOF of this circuit is

$$2^{m_{\text{bl}}} + 2^{2m_{\text{bl}} - 1}(dm_{\text{deg}} - m_{\text{bl}}). \quad (49)$$

We alternately optimize the blocks  $\{\tilde{V}^i\}$  in the similar way to Algorithm 1 so that  $\langle a | \tilde{a}' \rangle$  is maximized, where  $|\tilde{a}'\rangle :=$

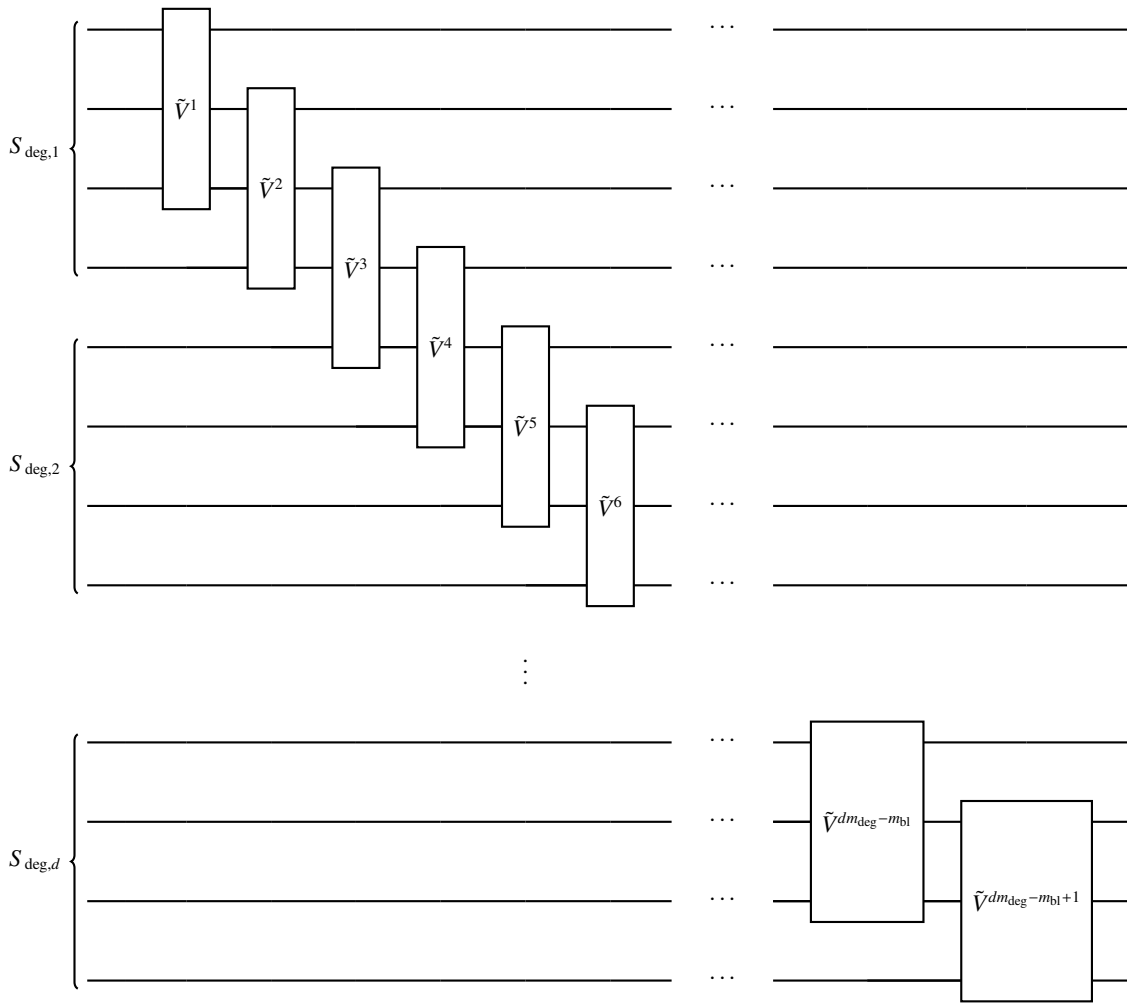


FIG. 4: The quantum circuit  $V'_{\text{MPS}}$  used in the additional numerical experiments in place of  $V_{\text{MPS}}$  for  $m_{\text{deg}} = 4$  and  $m_{\text{bl}} = 3$ .

$\sum_{\vec{l} \in [D]_0^d} \tilde{\alpha}'_l |l_1\rangle \cdots |l_d\rangle$  is the state generated by  $V'_{\text{MPS}}$ . Then, we get the approximation of  $V(0, \vec{s})$  as  $\tilde{f}'(\vec{s}) := \tilde{C} \sum_{\vec{l} \in [D]_0^d} \tilde{\alpha}'_l P_{\vec{l}}(\vec{s})$ .

In Fig. 5, we display the maximum difference of  $\tilde{f}'$  from the cosine expansion approximation on the diagonal line  $s_1 = \dots = s_d$ , taking  $m_{\text{bl}} = 2, \dots, 6$ , along with that of the MPS-based approximation. This figure shows that there is some power-law relationship between the approximation accuracy and the DOF in region with large DOF. This behavior is similar to that often observed in critical systems of MPS applied to one-dimensional quantum systems or two-dimensional classical systems[67–73]. If this behavior also appears in the case of  $d \gg 1$ , one might make a similar argument to the finite bond-dimension (entanglement) scaling refined in the study of MPS and evaluate  $\tilde{f}$  with an appropriate extrapolations with respect to DOF.

We also show the relationship between the accuracy of the cosine expansion approximation and its DOF in Fig. 5. We plot the maximum error of the approximated worst-of put option price by the cosine expansions of low degree  $D = 3, \dots, 10$

on the line  $s_1 = \dots = s_d$ , taking that of degree  $D = 16$  as the reference value. We see that the error of the low-degree cosine expansion is much larger than that of  $\tilde{f}'$  with comparable DOF. This result is another evidence of the advantage of our MPS-based approximation and the approximation by the circuit  $V'_{\text{MPS}}$  over the simple cosine expansion.

#### IV. SUMMARY

In this paper, we have considered how to extract the function encoded in the amplitudes of the quantum state as classical data. Such a task necessarily accompanies with quantum algorithms such as PDE solvers, but there has not been any proposal on the general way for it, despite its importance that it might ruin the quantum speedup. We have proposed the method based on orthogonal function expansion and tensor network. Orthogonal function expansion is widely used for function approximation, but suffers from the exponential increase of the number of the parameters, the expansion coefficient

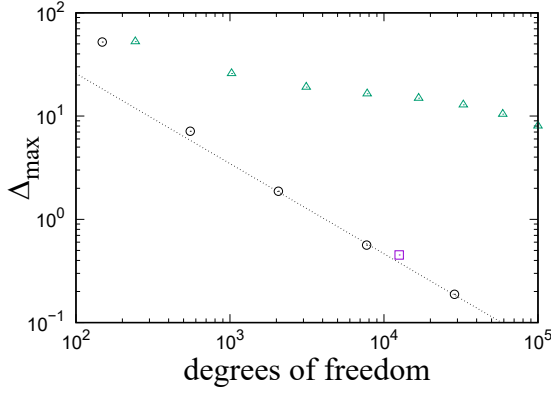


FIG. 5: The maximum difference  $\Delta_{\max}$  of the various approximations for the five-asset worst-of put option price from the cosine expansion approximation of degree  $D = 16$  on the line  $s_1 = \dots = s_5$ . The circles indicate those of the approximations based on the circuit  $V'_{\text{MPS}}$  in Fig. 4. From left to right, the points correspond to  $m_{\text{bl}} = 2, \dots, 6$ , respectively. The dotted line is the function  $\Delta_{\max}(x) = ax^b$  of the degrees of freedom  $x$  with  $a = e^{7.27}$  and  $b = -0.87$ , fitted with respect to the data for  $m_{\text{bl}} = 4, 5$ , and  $6$ . The square indicates the maximum difference of the MPS-based approximation. The triangles indicate those of the cosine expansion approximations of degree  $D = 3, \dots, 10$ , which corresponds to the points from left to right, respectively. The vertical and horizontal lines corresponds to the maximum difference and the DOF of the approximations, respectively.

cients, with respect to the dimension, that is, the number of the variables of the function. We then use a MPS, a kind of tensor network, to approximate the coefficients as the high-order tensor and reduce the DOF. We have presented the quantum circuit that produces the state corresponding to such a function approximation. Such a circuit is in fact constructible, since a MPS is encoded in a quantum state by a simple circuit, and so are orthogonal functions because of their orthogonal relation. We have also presented the procedure to optimize the quantum circuit and the MPS-based approximation, based on the alternating method proposed in [56]. Finally, we have conducted the numerical experiment to approximate finance-motivated multivariate function and found that our method works in this case.

We expect that the proposed method can be widely used in combination with various quantum algorithms that output function-encoding states, whether they are FTQC algorithms or NISQ ones. In future works, we will try to combine this method with concrete function finding quantum algorithms on concrete problems and present the complete set of the algorithms, along with more quantitative analysis of complexity.

#### ACKNOWLEDGEMENT

This work is partially supported by KAKENHI Grant Numbers JP22K11924, JP21H04446, JP21H05182, and JP21H05191 from JSPS of Japan. It is also supported by JST

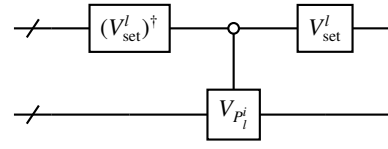


FIG. 6: The implementation of  $V'_{P_i}$  in Eq. (A3). The open circle represents the control on the gate  $V_{P_i}$  such that it is activated if and only if all the qubits in the first register take  $|0\rangle$ .

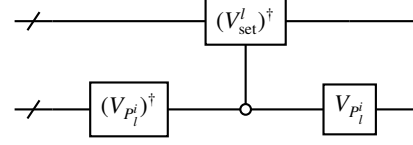


FIG. 7: The implementation of  $V^{i,l}_{\text{reset}}$  in Eq. (A6).

PRESTO No. JPMJPR1911, MEXT Q-LEAP Grant No. JPMXS0120319794, and JST COI-NEXT No. JPMJPF2014. H.U was supported by the COE research grant in computational science from Hyogo Prefecture and Kobe City through Foundation for Computational Science.

#### Appendix A: How to construct $V^i_{\text{OF}}$

To implement  $V^i_{\text{OF}}$  in Eq. (9), we need some building-block quantum gates. First, for any  $i \in [d]$  and  $l \in [D]_0$ , we assume the availability of the gate  $V_{P_i}$  that acts on a  $m_{\text{gr}}$ -qubit register as

$$V_{P_i} |0\rangle = |P_i^i\rangle, \quad (\text{A1})$$

where  $|P_i^i\rangle$  is given in Eq. (9). In fact, commonly used orthogonal functions such as trigonometric functions and orthogonal polynomials are explicitly given as elementary functions, and thus the state generation oracle like Eq. (A1) is constructed by the so-called Grover-Rudolph method [74, 75]. Second, for any  $n \in \mathbb{N}_0$ , we denote by  $V_{\text{set}}^n$  the gate that acts on a quantum register having the sufficient number of qubits as

$$V_{\text{set}}^n |0\rangle = |n\rangle. \quad (\text{A2})$$

This can be constructed by putting the Pauli-X gate (resp. nothing) on the  $a$ th qubit in the register if the binary representation of  $n$  has 1 (resp. 0) at the  $a$ th digit.

Then, for any  $i \in [d]$  and  $l \in [D]_0$ , using the controlled  $V_{P_i}$  and  $V'_{\text{set}}$ , we can implement the following gate on the system of two  $m_{\text{gr}}$ -qubit registers

$$V'_{P_i} := |l\rangle\langle l| \otimes V_{P_i} + \sum_{l' \in [n_{\text{gr}}]_0 \setminus \{l\}} |l'\rangle\langle l'| \otimes I, \quad (\text{A3})$$

where  $I$  is the identity operator, as shown in Fig. 6. Combining the gates of this type, we obtain

$$V^i_{\text{OF}} := \prod_{l=0}^{D-1} V'_{P_i} = \sum_{l=0}^{D-1} |l\rangle\langle l| \otimes V_{P_i} + \sum_{l=D}^{n_{\text{gr}}-1} |l\rangle\langle l| \otimes I, \quad (\text{A4})$$

which acts as

$$V_{\text{OF1}}^i |l\rangle |0\rangle = |l\rangle |P_l^i\rangle \quad (\text{A5})$$

for any  $l \in [D]_0$ .

Besides, for any  $i \in [d]$  and  $l \in [D]_0$ , using the controlled  $V_{\text{set}}^l$  and  $V_{P_l^i}$ , we construct the following gate on the system of two  $m_{\text{gr}}$ -qubit registers

$$V_{\text{reset}}^{i,l} := (V_{\text{set}}^l)^\dagger \otimes |P_l^i\rangle \langle P_l^i| + \sum_{|\psi_\perp\rangle} I \otimes |\psi_\perp\rangle \langle \psi_\perp|. \quad (\text{A6})$$

Here, in the second term of the RHS,  $|\psi_\perp\rangle$  runs over the  $n_{\text{gr}} - 1$  states that constitute the orthonormal basis of  $H$ , the Hilbert space on the  $m_{\text{gr}}$ -qubit register, in combination with  $|P_l^i\rangle$ . The concrete implementation is as shown in Fig. 7. Note that, in the circuit in this figure,  $(V_{\text{set}}^l)^\dagger$  is activated if the second reg-

ister takes  $|P_l^i\rangle$  but not activated if it takes the state  $|\psi\rangle$  orthogonal to  $|P_l^i\rangle$ , since  $(V_{P_l^i})^\dagger |\psi\rangle$  is orthogonal to  $(V_{P_l^i})^\dagger |P_l^i\rangle = |0\rangle$ . We then get

$$V_{\text{OF2}}^i := \prod_{l=0}^{D-1} V_{\text{reset}}^{i,l} = \sum_{l=0}^{D-1} (V_{\text{set}}^l)^\dagger \otimes |P_l^i\rangle \langle P_l^i| + \sum_{|\psi_\perp\rangle} I \otimes |\psi_\perp\rangle \langle \psi_\perp|, \quad (\text{A7})$$

where, in the second sum,  $|\psi_\perp\rangle$  runs over the  $n_{\text{gr}} - D$  states that constitute the orthonormal basis of  $H$  in combination with  $|P_0^i\rangle, \dots, |P_{D-1}^i\rangle$ .

Note that, for any  $l \in [D]_0$ ,

$$V_{\text{OF2}}^i V_{\text{OF1}}^i |l\rangle |0\rangle = |0\rangle |P_l^i\rangle \quad (\text{A8})$$

holds. Therefore,  $V_{\text{OF2}}^i V_{\text{OF1}}^i$  with a SWAP gate added at last is  $V_{\text{OF}}^i$ , with the second register deemed ancillary one.

- 
- [1] A. W. Harrow, A. Hassidim, and S. Lloyd, *Phys. Rev. Lett.* **103**, 150502 (2009).
- [2] A. Ambainis, in *STACS'12 (29th Symposium on Theoretical Aspects of Computer Science)*, Vol. 14 (LIPIcs, 2012) pp. 636–647.
- [3] B. D. Clader, B. C. Jacobs, and C. R. Sprouse, *Phys. Rev. Lett.* **110**, 250504 (2013).
- [4] A. M. Childs, R. Kothari, and R. D. Somma, *SIAM Journal on Computing* **46**, 1920 (2017).
- [5] S. Chakraborty, A. Gilyén, and S. Jeffery, in *46th International Colloquium on Automata, Languages, and Programming (ICALP 2019)* (Schloss Dagstuhl-Leibniz-Zentrum fuer Informatik, 2019).
- [6] Y. Subaşı, R. D. Somma, and D. Orsucci, *Phys. Rev. Lett.* **122**, 060504 (2019).
- [7] L. Lin and Y. Tong, *Quantum* **4**, 361 (2020).
- [8] Y. Tong, D. An, N. Wiebe, and L. Lin, *Phys. Rev. A* **104**, 032422 (2021).
- [9] D. An and L. Lin, *ACM Transactions on Quantum Computing* **3**, 5 (2022).
- [10] P. Costa, D. An, Y. R. Sanders, Y. Su, R. Babbush, and D. W. Berry, *arXiv preprint arXiv:2111.08152* (2021).
- [11] D. W. Berry, *Journal of Physics A: Mathematical and Theoretical* **47**, 105301 (2014).
- [12] D. W. Berry, A. M. Childs, A. Ostrander, and G. Wang, *Communications in Mathematical Physics* **356**, 1057 (2017).
- [13] A. M. Childs and J.-P. Liu, *Communications in Mathematical Physics* **375**, 1427 (2020).
- [14] T. Xin, S. Wei, S. Cui, J. Xiao, I. Arrazola, L. Lamata, X. Kong, D. Lu, E. Solano, and G. Long, *Phys. Rev. A* **101**, 032307 (2020).
- [15] Y. Cao, A. Papageorgiou, I. Petras, J. Traub, and S. Kais, *New J. Phys.* **15**, 013021 (2013).
- [16] A. Montanaro and S. Pallister, *Phys. Rev. A* **93**, 032324 (2016).
- [17] P. C. S. Costa, S. Jordan, and A. Ostrander, *Phys. Rev. A* **99**, 012323 (2019).
- [18] A. M. Childs, J.-P. Liu, and A. Ostrander, *Quantum* **5**, 574 (2021).
- [19] N. Linden, A. Montanaro, and C. Shao, *Communications in Mathematical Physics* (2022).
- [20] J.-P. Liu, H. O. Kolden, H. K. Krovi, N. F. Loureiro, K. Trivisa, and A. M. Childs, *Proceedings of the National Academy of Sciences* **118**, e2026805118 (2021).
- [21] C. Xue, Y.-C. Wu, and G.-P. Guo, *New J. Phys.* **23**, 123035 (2021).
- [22] S. Lloyd, G. De Palma, C. Gokler, B. Kiani, Z.-W. Liu, M. Marvian, F. Tennie, and T. Palmer, *arXiv preprint arXiv:2011.06571* (2020).
- [23] H. Krovi, *arXiv preprint arXiv:2202.01054* (2022).
- [24] S. Jin and N. Liu, *arXiv preprint arXiv:2202.07834* (2022).
- [25] D. An, D. Fang, S. Jordan, J.-P. Liu, G. H. Low, and J. Wang, *arXiv preprint arXiv:2205.01141* (2022).
- [26] B. T. Kiani, G. De Palma, D. Englund, W. Kaminsky, M. Marvian, and S. Lloyd, *Phys. Rev. A* **105**, 022415 (2022).
- [27] K. Miyamoto and K. Kubo, *IEEE Transactions on Quantum Engineering* **3**, 3100225 (2021).
- [28] S. Endo, J. Sun, Y. Li, S. C. Benjamin, and X. Yuan, *Phys. Rev. Lett.* **125**, 010501 (2020).
- [29] M. Lubasch, J. Joo, P. Moinier, M. Kiffner, and D. Jaksch, *Phys. Rev. A* **101**, 010301 (2020).
- [30] H.-L. Liu, Y.-S. Wu, L.-C. Wan, S.-J. Pan, S.-J. Qin, F. Gao, and Q.-Y. Wen, *Phys. Rev. A* **104**, 022418 (2021).
- [31] Y. Sato, R. Kondo, S. Koide, H. Takamatsu, and N. Imoto, *Phys. Rev. A* **104**, 052409 (2021).
- [32] F. Fontanela, A. Jacquier, and M. Oumgari, *SIAM Journal on Financial Mathematics* **12**, SC98 (2021).
- [33] O. Kyriienko, A. E. Paine, and V. E. Elfving, *Phys. Rev. A* **103**, 052416 (2021).
- [34] F. Y. Leong, E. W.-B., and D. E. Koh, *Scientific Reports* **12**, 10817 (2022).
- [35] P. García-Molina, J. Rodríguez-Mediavilla, and J. J. García-Ripoll, *Phys. Rev. A* **105**, 012433 (2022).
- [36] H. Alghassi, A. Deshmukh, N. Ibrahim, N. Robles, S. Woerner, and C. Zoufal, *Quantum* **6**, 730 (2022).
- [37] J. Gonzalez-Conde, Á. Rodríguez-Rozas, E. Solano, and M. Sanz, *arXiv preprint arXiv:2101.04023* (2021).
- [38] S. K. Radha, *arXiv preprint arXiv:2101.04280* (2021).
- [39] J. Joo and H. Moon, *arXiv preprint arXiv:2109.09216* (2021).
- [40] A. E. Paine, V. E. Elfving, and O. Kyriienko, *arXiv preprint arXiv:2203.08884* (2022).
- [41] K. Kubo, K. Miyamoto, K. Mitarai, and K. Fujii, *arXiv preprint arXiv:2207.01277* (2022).

- [42] Y. Liu, Z. Chen, C. Shu, S. C. Chew, and B. C. Khoo, [arXiv preprint arXiv:2207.14630](#) (2022).
- [43] S. Aaronson, *Nature Physics* **11**, 291 (2015).
- [44] G. Brassard, P. Hoyer, M. Mosca, and A. Tapp, *Contemporary Mathematics* **305**, 53 (2002).
- [45] Y. Suzuki, S. Uno, R. Raymond, T. Tanaka, T. Onodera, and N. Yamamoto, *Quantum Inf. Process.* **19**, 75 (2020).
- [46] R. Orús, *Annals of physics* **349**, 117 (2014).
- [47] K. Okunishi, T. Nishino, and H. Ueda, *Journal of the Physical Society of Japan* **91**, 062001 (2022).
- [48] A. Nouy, *Model Reduction and Approximation: Theory and Algorithms* **15**, 3672148 (2017).
- [49] M. Griebel and H. Harbrecht, *Foundations of Computational Mathematics*, **1** (2021).
- [50] M. Ali and A. Nouy, [arXiv preprint arXiv:2007.00118](#) (2020).
- [51] M. Ali and A. Nouy, [arXiv preprint arXiv:2007.00128](#) (2020).
- [52] M. Ali and A. Nouy, [arXiv preprint arXiv:2101.11932](#) (2021).
- [53] M. Bachmayr, A. Nouy, and R. Schneider, [arXiv preprint arXiv:2112.01474](#) (2021).
- [54] M. Griebel, H. Harbrecht, and R. Schneider, [arXiv preprint arXiv:2203.04100](#) (2022).
- [55] S.-J. Ran, *Phys. Rev. A* **101**, 032310 (2020).
- [56] T. Shirakawa, H. Ueda, and S. Yunoki, [arXiv preprint arXiv:2112.14524](#) (2021).
- [57] L. Zhizhiashvili, *Trigonometric Fourier series and their conjugates*, Vol. 372 (Springer Science & Business Media, 1996).
- [58] L. N. Trefethen, *Approximation Theory and Approximation Practice, Extended Edition* (SIAM, 2019).
- [59] S. Holtz, T. Rohwedder, and R. Schneider, *SIAM Journal on Scientific Computing* **34**, A683 (2012).
- [60] J. C. Hull, *Options futures and other derivatives* (Pearson, 2003).
- [61] S. E. Shreve, *Stochastic calculus for finance I & II* (Springer, 2004).
- [62] M. Scholes and F. Black, *Journal of Political Economy* **81**, 637 (1973).
- [63] R. C. Merton, *The Bell Journal of Economics and Management Science* **4**, 141 (1973).
- [64] <https://github.com/google/tf-quant-finance>.
- [65] R. Kangro and R. Nicolaidis, *SIAM Journal on Numerical Analysis* **38**, 1357 (2000).
- [66] M. Fishman, S. R. White, and E. M. Stoudenmire, *SciPost Phys. Codebases*, **4** (2022).
- [67] T. Nishino, K. Okunishi, and M. Kikuchi, *Physics Letters A* **213**, 69 (1996).
- [68] L. Tagliacozzo, T. R. de Oliveira, S. Iblisdir, and J. I. Latorre, *Phys. Rev. B* **78**, 024410 (2008).
- [69] F. Pollmann, S. Mukerjee, A. M. Turner, and J. E. Moore, *Phys. Rev. Lett.* **102**, 255701 (2009).
- [70] B. Pirvu, G. Vidal, F. Verstraete, and L. Tagliacozzo, *Phys. Rev. B* **86**, 075117 (2012).
- [71] J. A. Kjäll, M. P. Zaletel, R. S. K. Mong, J. H. Bardarson, and F. Pollmann, *Phys. Rev. B* **87**, 235106 (2013).
- [72] V. Stojevic, J. Haegeman, I. P. McCulloch, L. Tagliacozzo, and F. Verstraete, *Phys. Rev. B* **91**, 035120 (2015).
- [73] H. Ueda, K. Okunishi, R. Krčmár, A. Gendiar, S. Yunoki, and T. Nishino, *Phys. Rev. E* **96**, 062112 (2017).
- [74] L. Grover and T. Rudolph, [arXiv preprint quant-ph/0208112](#) (2002).
- [75] K. Kaneko, K. Miyamoto, N. Takeda, and K. Yoshino, *EPJ Quantum Technology* **9**, 7 (2022).